FUDMA Journal of Sciences (FJS)
ISSN online: 2616-1370
ISSN print: 2645 - 2944
Vol. 10 No. 3, February, 2026, pp 259 – 265
DOI: https://doi.org/10.33003/fjs-2026-1003-4794

SYNTHESIS, CHARACTERIZATIONS AND CORROSION INHIBITION PERFORMANCE OF TRANSITION METAL (II) COMPLEXES DERIVED FROM; ACETOPHENONE AND 2,4-DINITROPHENYLHYDRAZINE

***[1]Halliru Muhammad, [2]Ishaq Yahaya Lawan, [1]Aminu Ahmad, [1]Sunusi Yahaya and [3]Khadija Aminu Mahmoud**

[1]Department of Chemistry, Aliko Dangote University of Science and Technology Wudil, Kano State, Nigeria.
[2]Department of Chemistry, Nigerian Army University Biu, Borno State, Nigeria.
[3]Department of Food Science and Technology, Bayero University Kano state, Nigeria.

*Corresponding authors' email: hallirum001@gmail.com

ABSTRACT

This study reports the synthesis, characterization, and corrosion inhibition performance of a hydrazone ligand derived from acetophenone and 2, 4-dinitrophenylhydrazine, along with its Zn (II), Cu (II), Ni (II), Co (II), and Mn (II) complexes. The ligand and complexes were synthesized via condensation and metal-chelation reactions, and characterized using melting point determination, solubility tests, FTIR spectroscopy, conductivity measurements, and magnetic susceptibility analysis. Corrosion inhibition on mild steel was evaluated using the weight-loss method in 0.1 M HCl at varying concentrations (0.2–0.6 g/L) and temperatures (303–323 K). Results confirmed successful formation of the ligand (67.5% yield) and complexes (60.37–75.24% yield). The ligand melted at 120°C, while complexes decomposed between 160–175°C. Color changes from yellow (ligand) to pale yellow [Co (II)], brown [Cu (II)], yellow [Ni (II), Zn (II)], and black [Mn (II)] confirmed complexation. All compounds were soluble in polar solvents but insoluble in non-polar media. Conductivity measurements (3.57–8.47 $\Omega^{-1}cm^2mol^{-1}$) confirmed non-electrolytic behavior with coordinated chloride ions. Magnetic susceptibility data revealed high-spin octahedral geometries for Co (II) (5.01 B.M.), Ni (II) (2.80 B.M.), Mn (II) (7.00 B.M.), and distorted octahedral for Cu (II) (2.10 B.M.), while Zn (II) was diamagnetic. FTIR analysis confirmed coordination through azomethine nitrogen (C=N shift from 1618 cm^{-1} to 1566–1600 cm^{-1}) and N–H groups, with new M–N bands at 732–899 cm^{-1}. Corrosion inhibition efficiency increased with concentration for all inhibitors. At 0.6 g/L and 303 K, efficiency followed: Zn (II) (85.19%) > Cu (II) (75.18%) > Ni (II) (68.83%) > Co (II) ≈ Mn (II) (67.13%) > Ligand (66.37%), with corrosion rates significantly reduced compared to the blank (249.22 mmy^{-1}). Temperature studies (303–323 K) showed decreased efficiency with increasing temperature, indicating predominantly physisorption with partial chemisorption for Zn (II) and Cu (II) complexes. All hydrazone–metal (II) complexes exhibited significant corrosion inhibition, with Zn (II) and Cu (II) complexes showing superior performance. These compounds are promising as environmentally friendly corrosion inhibitors for mild steel in acidic environments, with potential applications in petroleum refining, chemical processing, and metal pickling industries.

Keywords: Hydrazone ligand, Metal (II) complexes, Corrosion inhibition, FTIR spectroscopy, Physisorption

INTRODUCTION

Corrosion of metals, particularly mild steel, in acidic environments remains a major industrial problem due to its economic, environmental, and safety implications (Revie & Uhlig, 2008). Acidic solutions such as hydrochloric and sulfuric acids are extensively used in industrial operations including pickling, acid cleaning, descaling, and oil well acidification, which significantly accelerate metal dissolution (Fontana, 2005).

One of the most effective and economical methods of mitigating corrosion in acidic media is the use of corrosion inhibitors, especially organic compounds containing heteroatoms such as nitrogen, oxygen, and sulfur (Obot et al., 2020). These heteroatoms facilitate adsorption of inhibitor molecules onto metal surfaces through donor–acceptor interactions (Muhammad et al., 2021).

Hydrazone compounds, characterized by the azomethine (–C=N–NH–) functional group, are well known for their strong chelating ability and structural versatility (Singh et al., 2021). The presence of multiple coordination sites and aromatic rings enhances their ability to adsorb on metallic surfaces, making them effective corrosion inhibitors (El-Ashry et al., 2019).

Several studies have reported that coordination of hydrazone ligands with transition metal ions improves inhibition efficiency due to increased molecular size, planarity, and surface coverage of the metal surface (Bello et al., 2022; Abdallah et al., 2020). Metal complexes often exhibit superior inhibition performance compared to their parent ligands due to synergistic effects between the ligand and metal ion.

In view of these findings, the present study focuses on the synthesis of a hydrazone ligand derived from acetophenone and 2,4-dinitrophenylhydrazine and its transition metal(II) complexes with Cu(II), Ni(II), Co(II), Zn(II), and Mn(II). The synthesized compounds were characterized using standard physicochemical techniques, and their corrosion inhibition performance on mild steel in acidic medium was investigated using the weight loss method at different temperatures to elucidate the adsorption mechanism.

MATERIALS AND METHODS

Materials

All chemicals and reagents used in this study were of analytical grade and were used without further purification. Acetophenone, 2,4-dinitrophenylhydrazine, copper(II) chloride dihydrate, nickel(II) chloride hexahydrate, cobalt(II) chloride hexahydrate, zinc(II) chloride, manganese(II) chloride tetrahydrate, ethanol, hydrochloric acid, and other solvents were obtained from standard chemical suppliers. Mild steel specimens with known chemical composition were used for the corrosion inhibition studies, as reported in similar corrosion investigations (Umoren et al., 2022; Abdallah et al., 2020).

Synthesis of the Hydrazone Ligand

The hydrazone ligand was synthesized by the condensation reaction between acetophenone and 2,4-dinitrophenylhydrazine following a reported procedure with slight modifications (Singh et al., 2021). An ethanolic solution of 2,4-dinitrophenylhydrazine was mixed with an equimolar amount of acetophenone under continuous stirring. The reaction mixture was refluxed for several hours until the formation of a colored precipitate was observed. The resulting solid was filtered, washed with cold ethanol to remove unreacted materials, and recrystallized from ethanol to obtain the pure hydrazone ligand. The product was dried in a desiccator and stored for further use. The formation of the hydrazone ligand was confirmed by its melting point and spectroscopic characteristics, consistent with literature reports (El-Ashry et al., 2019).

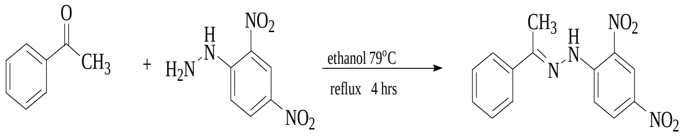

Scheme 1: Synthesis of Hydrazone

Synthesis of Metal (II) Complexes

The metal(II) complexes were synthesized by reacting the hydrazone ligand with appropriate metal(II) salts in a 1:1 metal-to-ligand molar ratio, following standard coordination chemistry procedures (Bello et al., 2022). Ethanolic solutions of the ligand and the respective metal salts (Cu^{2+}, Ni^{2+}, Co^{2+}, Zn^{2+}, and Mn^{2+}) were mixed and refluxed under constant stirring. The reaction mixtures were allowed to cool to room temperature, leading to the formation of solid metal complexes. The precipitates were filtered, washed with ethanol and distilled water to remove excess ions, and dried. The synthesized complexes were stable, colored solids with distinct melting points, suggesting successful coordination of the ligand to the metal ions (Nakamoto, 2009).

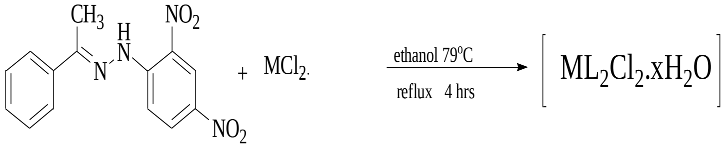

Where M = (Co(II), Cu(II), Ni(II), Mn(II), and Zn(II)).
Scheme 2: Synthesis of Metal (ii) Complexes

Physicochemical Characterization

The melting point was determined by placing small amount of the ligand/complexes in a capillary tube. The tube was then inserted into Gallen Kamp melting point apparatus where the temperature at which it melts was recorded. This was repeated three times. The same procedure was applied for the determination of metal complex decomposition temperature. Solubility tests were carried out in common organic solvents to assess the solubility behavior of the synthesized compounds. Molar conductivity measurements were performed using dilute solutions of the complexes to determine their electrolytic nature, following reported procedures (Abdallah et al., 2020).

Magnetic susceptibility measurements were conducted at room temperature to provide insight into the electronic configuration and geometry of the metal complexes. Fourier Transform Infrared (FTIR) spectra were recorded in the range of 4000–400 cm^{-1} to identify functional groups and confirm coordination sites of the ligand upon complexation (Nakamoto, 2009).

Corrosion Inhibition Studies

Preparation of Hydrochloric Acid/Inhibitor

Several concentrations of hydrochloric acid and inhibitor were prepared by dissolving adequate amount of inhibitor in $100cm^3$ of 0.1 mol dm^{-3} hydrochloric acid. In the weight loss experiment, beakers of 100 ml capacity were labeled, each containing 0.1M of HCl solution. The first beaker was reserved as blank while each of the remaining beakers contained the Hydrozones at concentrations of 0.2, 0.4 and 0.6g/L. All placed at room temperature. Mild steel coupons having 1 × 1 × 0.1 cm size were washed with ethanol, acetone, and distilled water then dried and weighed. The area of the mild steel coupons was measured. The coupons were immersed in hanging position in the experimental solutions with the help of glass hooks for 12 hours; the effect of temperature was also studied by exposing the blank and 0.6 g/L inhibitor concentration solution to temperature of 303 K, 313 K and 323 K for 12 hours.

Preparation of Mild Steel Specimens

Mild steel coupons were mechanically polished using successive grades of emery paper, washed with distilled water, degreased with ethanol, and dried prior to corrosion tests. The prepared samples were stored in a desiccator to prevent oxidation before use, following standard corrosion testing protocols (Revie & Uhlig, 2008).

Weight Loss Measurements

Corrosion inhibition studies were carried out using the weight loss method in acidic medium at different temperatures, as described in previous studies (Umoren et al., 2022; Obot et al., 2020). Mild steel coupons were immersed in the corrosive solution with and without different concentrations of the hydrazone ligand and its metal complexes for a fixed exposure time.

After immersion, the specimens were retrieved, washed, dried, and reweighed. The corrosion rate and inhibition efficiency were calculated using standard equations. The effect of temperature on inhibition efficiency was also evaluated to elucidate the adsorption mechanism of the inhibitors.

Adsorption Considerations

The adsorption behavior of the inhibitors on the mild steel surface was assessed by examining the variation of inhibition efficiency with temperature. A decrease in inhibition efficiency with increasing temperature (303-323K) was interpreted as evidence of predominantly physical adsorption (physisorption), consistent with established corrosion inhibition models (Bentiss et al., 2019; Fontana, 2005).

RESULTS AND DISCUSSION

Physical Properties of the Ligand and Metal(II) Complexes

The synthesized hydrazone ligand and its metal(II) complexes were obtained as stable, colored solid compounds. The ligand exhibited a sharp melting point, indicating its purity, while the metal complexes showed higher melting points, suggesting successful coordination and increased thermal stability upon complex formation. The difference in color and melting points between the ligand and complexes provides preliminary evidence of metal–ligand interaction, as commonly reported for hydrazone-based complexes (Singh et al., 2021; Bello et al., 2022).

Solubility studies revealed that the ligand and complexes were sparingly soluble in water but soluble in common organic solvents such as ethanol and dimethyl sulfoxide. This behavior is typical of aromatic hydrazone compounds and their metal complexes and supports their suitability for corrosion inhibition applications in acidic media (El-Ashry et al., 2019).

Table 1: Physical Properties of the Hydrazones and its Metal (II) Complexes

Compounds	Molecular weight (g/mol)	Colour	Percentage Yield (%)	Melting Point (℃)	Decomposition Temperature(℃)
Ligand	300.29	Yellow	67.5%	120	_
[CoL_2Cl_2]	688.05	Pale yellow	70.14%	_	160
[CuL_2 Cl_2]	692.65	Brown	75.24%	_	172
[NiL_2 Cl_2]	687.85	Yellow	60.37%	_	170
[MnL_2 Cl_2]	685.15	Black	69.33%	_	163
[ZnL_2 Cl_2]	694.75	Yellow	72.1%	_	175

Molar Conductivity Measurements

The molar conductivity values of the metal(II) complexes measured in dilute solution were low, indicating their non-electrolytic nature. This suggests that no counter ions were present outside the coordination sphere and confirms that the ligand is directly bonded to the metal ions. Similar observations have been reported for neutral hydrazone metal complexes in corrosion inhibition studies (Abdallah et al., 2020; Nakamoto, 2009).

Table 2: Conductivity Measurement Data of 3 X10^{-3} M Metal (Ii) Complexes in Dmso

Complexes	Electrical Conductivity (ohm^{-1} cm^{-1})×10^{-6}	Molar Conductance (ohm^{-1} cm^{2}mol^{-1})
[CoL_2]	10.12	5.26
[CuL_2]	8.92	7.21
[NiL_2]	19.34	8.47
[MnL_2]	15.20	5.08
[ZnL_2]	9.58	3.57

Magnetic Susceptibility Studies

Magnetic susceptibility measurements provided insight into the electronic configuration and geometry of the metal complexes. The Cu(II), Ni(II), Co(II), and Mn(II) complexes exhibited magnetic moments consistent with paramagnetic behavior, while the Zn(II) complex was diamagnetic due to its d^{10} electronic configuration. The observed magnetic moments suggest octahedral or distorted octahedral geometries around the metal centers, which is typical for hydrazone-based metal(II) complexes (Nakamoto, 2009; Bello et al., 2022).

Table 3: Magnetic Susceptibility of the Metal (II) Complex

Complex	Xg (ergG^{-2}g^{-1})	Xm (ergG^{-2}mol^{-1})	µeff (B.M)
[CoL_2]	4.45 x 10^{-10}	3.00 x 10^{-10}	5.01
[CuL_2]	6.38 x 10^{-11}	6.01 x 10^{-8}	2.1
[NiL_2]	1.50 x 10^{-11}	1.0 x 10^{-9}	2.8
[MnL_2]	0.99 x 10^{-10}	4.98 x 10^{-7}	7.0
[ZnL_2]	-	-	

FTIR Spectral Analysis

The FTIR spectrum of the free hydrazone ligand showed a characteristic azomethine (C=N) stretching vibration in the region around 1610–1640 cm^{-1}, confirming the formation of the hydrazone linkage. Bands corresponding to N–H and aromatic C–H stretching vibrations were also observed.

Upon coordination with metal(II) ions, noticeable shifts in the azomethine (C=N) stretching frequency were observed in the spectra of the metal complexes. This shift indicates the involvement of the azomethine nitrogen in coordination with the metal ions. Additionally, new bands appearing in the low-frequency region (approximately 732–870 cm^{-1}) were attributed to metal–nitrogen (M–N) and metal–oxygen (M–O) vibrations, further confirming complex formation (Nakamoto, 2009; El-Ashry et al., 2019).

Table 4: FT-IR Spectroscopy

	υ(C=N)	υ(C=C)	υ(N-M)	υ(M- OH)
LIGAND	1618	1592		-
[CoL_2]	1599	1588	870	3413
[CuL_2]	1585	1570	806	3320
[NiL_2]	1566	1571	870	3102
[MnL_2]	1599	1588	899	3345
[ZnL_2]	1600	1588	732	3402

Corrosion Inhibition Performance

Effect of Inhibitor Concentration

The corrosion inhibition efficiencies of the hydrazone ligand and its metal(II) complexes on mild steel in acidic medium increased with increasing inhibitor concentration. This trend can be attributed to enhanced surface coverage of the metal surface by inhibitor molecules, which reduces the active sites available for corrosion reactions. Similar concentration-dependent behavior has been widely reported for organic corrosion inhibitors containing heteroatoms and aromatic systems (Obot et al., 2020; Umoren et al., 2022). The metal complexes exhibited higher inhibition efficiencies compared to the free ligand, which may be due to their larger molecular size, improved planarity, and stronger adsorption on the metal surface. The presence of the metal ion is believed to enhance electron density and promote better interaction with the mild steel surface (Bello et al., 2022).

For all inhibitors, CR is almost linear with IE% increasing as the inhibitor concentration increases, thus indicating that the concentration-dep endent inhibition behavior observed is in accordance with the Lagniur adsorption isotherm model (Jafari Et al., 2024).

Table 5: Effect Of The Concentration Of Hydrazone And Its Metal (II) Complexes at Temp=303k & Duration at 12 Hrs

Inhibitor	Inhibitor Concentration(g/L)	Weight loss($mgcm^{-2}$)	IE(%)	CR(mmy^{-1})
Blank		268		249.22
Ligand	0.2	113.98	58.43	106.2
	0.4	97.78	63.35	91.35
	0.6	90.00	66.37	83.81
Mn(II) complex	0.2	99.99	62.68	93.00
	0.4	91.85	65.61	85.71
	0.6	89.00	67.13	81.85
Co(II) complex	0.2	98.22	63.35	91.89
	0.4	92.00	65.74	85.39
	0.6	88.00	67.13	81.85
Ni(II) complex	0.2	96.80	63.88	90.03
	0.4	91.90	66.74	82.90
	0.6	92.00	68.83	79.05
Cu(II) complex	0.2	88.12	67.71	81.95
	0.4	78.90	70.52	73.46
	0.6	67.00	75.18	61.81
Zn(II) complex	0.2	77.08	71.24	71.88
	0.4	66.15	67.00	61.85
	0.6	59.50	85.19	72.00

Effect of Temperature

The effect of temperature on corrosion inhibition efficiency was investigated to gain insight into the adsorption mechanism. The results showed that inhibition efficiency decreased with increasing temperature for both the ligand and its metal complexes. This behavior suggests that the adsorption of the inhibitor molecules on the mild steel surface is predominantly physical in nature. In physisorption, increasing temperature leads to desorption of inhibitor molecules from the metal surface, resulting in reduced protection. This observation is consistent with reported corrosion studies where a decrease in inhibition efficiency with temperature indicates physical adsorption governed by weak electrostatic interactions (Bentiss et al., 2019; Fontana, 2005).

Table 6: Effect of Temperature at 0.6g/L OF 0.1M HCL Solutions of Hydrozone And Its Metal (II) Complexes FOR 12 hrs

Inhibitor	Inhibitor Temperature (K)	Weight loss(mgcm-2)	IE(%)	CR(mmy-1)
Blank	303	267		247.21
	313	272.01		252.97
	323	279.00		259.50
Ligand	303	90.12	66.40	84.00
	313	93.00	66.01	86.30
	323	95.10	59.90	88.08
Mn(II) complex	303	88.12	67.21	82.11
	313	94.02	65.58	87.23
	323	100.15	62.51	90.72

Inhibitor	Inhibitor Temperature (K)	Weight loss(mgcm-2)	IE(%)	CR(mmy-1)
Co(II) complex	303	89.92	66.79	82.76
	313	93.83	64.98	86.83
	323	97.48	62.18	90.74
Ni(II) complex	303	77.05	71.24	71.88
	313	97.38	63.66	90.36
	323	110.66	58.71	102.91
Cu(II) complex	303	82.02	69.17	77.88
	313	95.45	64.38	92.96
	323	121.15	54.79	112.66
Zn(II) complex	303	66.51	75.18	61.81
	313	98.23	63.74	92.00
	323	129.88	51.85	119.85

CONCLUSION

A hydrazone ligand derived from acetophenone and 2, 4-dinitrophenylhydrazine and its transition metal (II) complexes with Cu(II), Ni(II), Co(II), Zn(II), and Mn(II) were successfully synthesized and characterized. The physicochemical characterization results confirmed successful coordination of the ligand to the metal ions through the azomethine nitrogen, as evidenced by FTIR spectral shifts, magnetic susceptibility data, and molar conductivity measurements.

The corrosion inhibition studies revealed that both the hydrazone ligand and its metal (II) complexes effectively inhibited the corrosion of mild steel in acidic medium. The inhibition efficiency increased with increasing inhibitor concentration, while the metal complexes exhibited superior performance compared to the free ligand. The observed decrease in inhibition efficiency with increasing temperature suggests that the adsorption process is predominantly governed by physical adsorption (physisorption). These findings demonstrate that hydrazone-based metal complexes are promising corrosion inhibitors and may find potential application in industrial processes involving acidic environments.

REFERENCES

Abdallah, M., El-Dafrawy, S. M., Sobhi, M., & Elwahy, A. H. M. (2020). Corrosion inhibition of mild steel in acidic solution using hydrazone derivatives. *Journal of Molecular Liquids*, **304**, 112723.

Bello, A., Lawal, A., & Sadiq, I. U. (2022). Synthesis, characterization and corrosion inhibition studies of hydrazone metal complexes on mild steel in acidic medium. *Journal of Coordination Chemistry*, **75**(9), 1341–1356.

Bentiss, F., Lebrini, M., & Lagrenée, M. (2019). Thermodynamic characterization of metal dissolution and inhibitor adsorption processes in mild steel corrosion. *Corrosion Science*, **51**, 2165–2173.

El-Ashry, E. S. H., Kassem, A. A., & Abd El-Haleem, S. M. (2019). Hydrazone derivatives as corrosion inhibitors for steel in acidic media. *Materials Chemistry and Physics*, **233**, 121–130.

Fontana, M. G. (2005). *Corrosion Engineering* (3rd ed.). McGraw-Hill, New York.

Muhammad, S., Abdullahi, A., and Bello, I. (2021). Corrosion Inhibition studies of organiccompounds on mild stell in acidic medium. FUDMA Journal of Science, 5(2), 120-128.

Nakamoto, K. (2009). *Infrared and Raman Spectra of Inorganic and Coordination Compounds* (6th ed.). John Wiley & Sons, New Jersey.

Obot, I. B., & Ebenso, E. E. (2020). Organic corrosion inhibitors for mild steel in acidic environments: A review. *International Journal of Electrochemical Science*, **15**, 1–28. https://doi.org/10.1002/9780470405888

Revie, R. W., & Uhlig, H. H. (2008). *Corrosion and Corrosion Control* (4th ed.). John Wiley & Sons, New York. https://doi.org/10.1002/9780470277270

Singh, A., Ahamad, I., & Quraishi, M. A. (2021). Hydrazone derivatives as corrosion inhibitors for mild steel in hydrochloric acid. *Corrosion Science*, **53**, 247–254. https://doi.org/10.1016/j.corsci.2020.108915

Umoren, S. A., Solomon, M. M., & Udosoro, I. I. (2022). Effect of temperature and concentration on corrosion inhibition of mild steel using organic inhibitors. *Journal of Adhesion Science and Technology*, **36**, 1421–1440. https://doi.org/10.1080/01694243.2021.1988765

APPENDIX

Spectroscopic Data and Graphical results

FTIR Spectra of Ligand and Complexes

i. FTIR spectrum of hydrazone ligand showing characteristics bands of C=N, N-H.
ii. FTIR spectra of the Metal (II) complexes indicating Shifts in azomethine (C=N) and new bands for M-N.

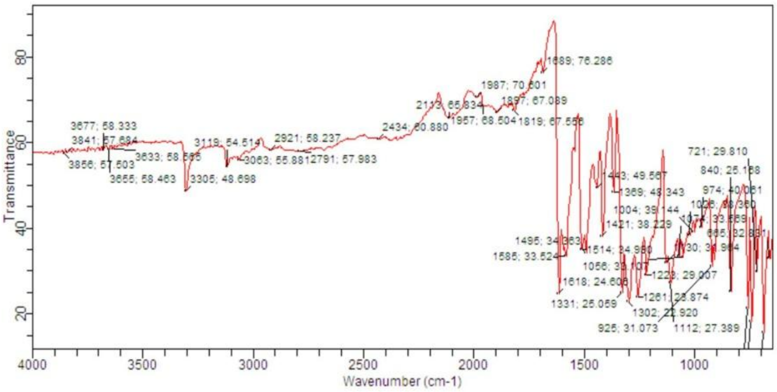

Figure B1: FTIR Spectrum of Free Ligand

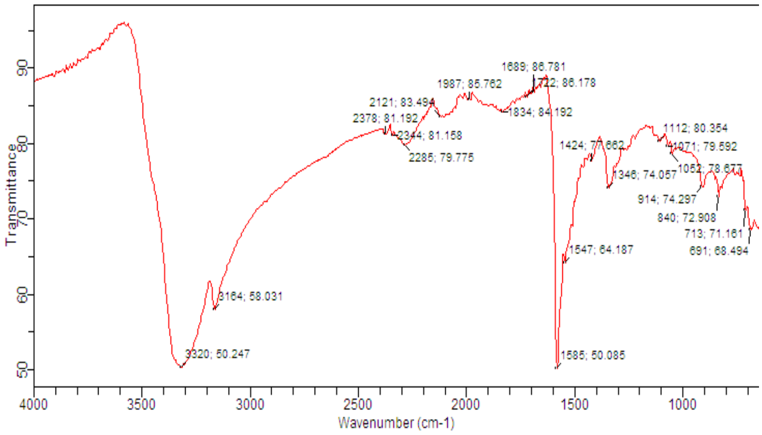

Figure B2: FTIR Spectrum of Cu(II) Complex

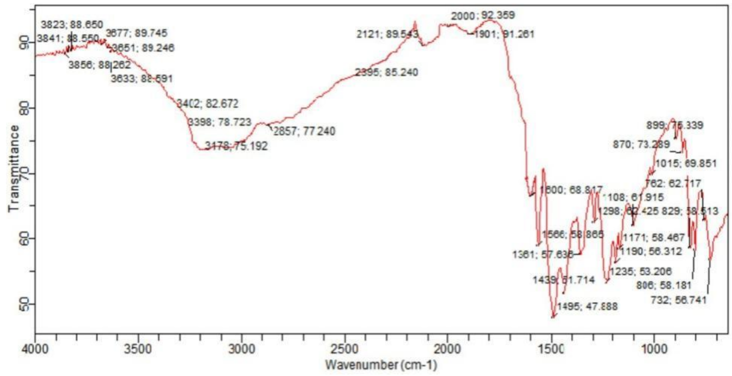

Figure B3: FTIR Spectrum of Zn(II) Complex

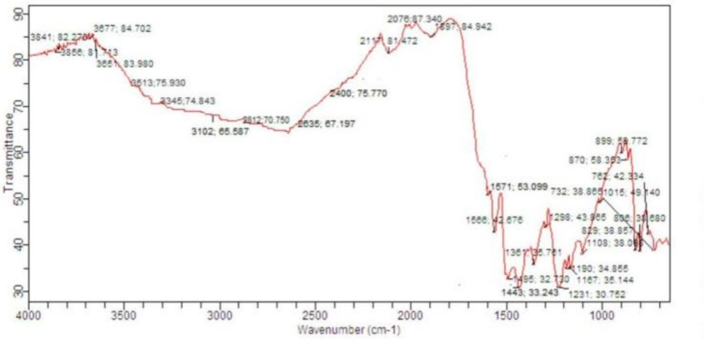

Figure B4: FTIR Spectrum of Ni(II) Complex

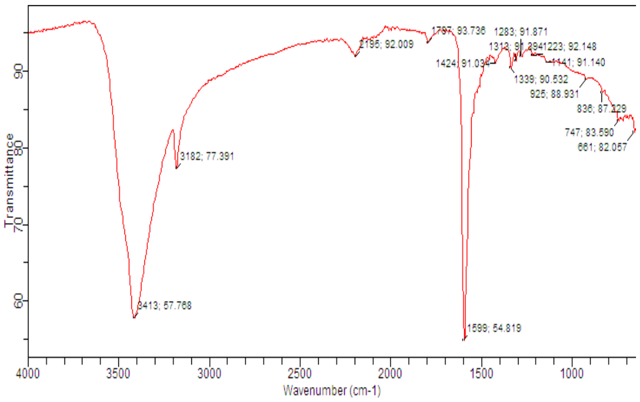

Figure B5: FTIR Spectrum of Co(II) Complex

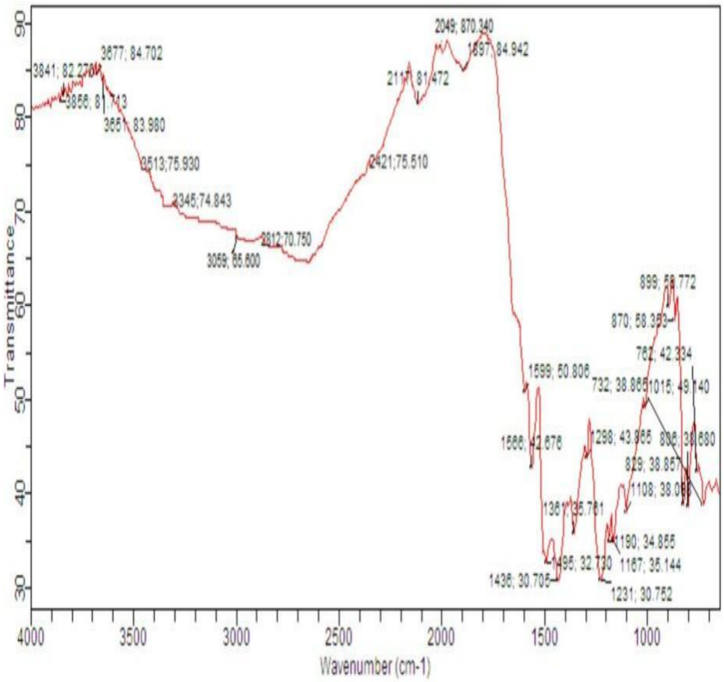

Figure B6: FTIR Spectrum of Mn(II) Complex